Title
INSTRUMENTATION FOR ENERGY DISPERSIVE X-RAY FLUORESCENCE

Author
Jaklevic, Joseph M.

Publication Date
1978-06-01

Submitted to the CRC Press, Inc.,
for book to be published in 1979.

INSTRUMENTATION FOR ENERGY DISPERSIVE X-RAY FLOURESCENCE

Joseph M. Jaklevic and Fred S. Goulding

June 1978

Prepared for the U. S. Department of Energy
under Contract W-7405-ENG-48

DISCLAIMER

Submitted to the CRC Press, Inc.,
for book to be published in 1979.

LBL-7997

INSTRUMENTATION FOR ENERGY DISPERSIVE X-RAY FLUORESCENCE

Joseph M. Jaklevic and Fred S. Goulding

June, 1978

Prepared for the U. S. Department of Energy
under Contract W-7405-ENG-48

CHAPTER 2

INSTRUMENTATION FOR ENERGY DISPERSIVE X-RAY FLUORESCENCE

Joseph M. Jaklevic and Fred S. Goulding

Department of Instrument Techniques
Lawrence Berkeley Laboratory
University of California
Berkeley, California 94720 U.S.A.

June 1978

I. INTRODUCTION

X-ray fluorescence analysis depends on illuminating a sample with radiation of an energy and type adequate to produce inner shell vacancies in the sample atoms. These vacancies then de-excite to produce x-rays whose energies are characteristics of the elements in the sample. The energy distribution of x-rays emitted from the sample can then be related to the concentrations of the elements present.

The energies of x-rays normally encountered in x-ray fluorescence analysis range from approximately 1 keV to 40 keV. For x-rays below 1 keV, the attenuation problems become so severe that accurate quantitative analysis becomes extremely difficult. For energies above 40 keV, excitation of characteristic K-shell fluorescence becomes improbable; consequently, L x-rays, which occur at low energies, are generally used for the heavier elements.

The viability of the XRF method depends upon the availability of a detector system which can measure the energies and intensities of x-rays in this energy region. It must exhibit an energy resolution adequate to distinguish one element from the next one in the periodic table and, ideally, to reduce the number of ambiguous overlaps of spectral lines to a minimum. During most of the history of x-ray fluorescence analysis, spectra were measured using crystal spectrometers which depend on the Bragg reflection of x-rays from regular, periodic lattices. A beam of x-rays incident at an angle θ with respect to a regular crystal surface will be reflected if the wavelength λ satisfies the following condition:

$$\lambda = 2d \sin \theta \tag{2.1}$$

where d is the spacing between lattice planes in the crystal. By limiting the range of incident angles and counting the number of reflected

x-rays as a function of angle of incidence, the spectral distribution of the radiation is determined. The wavelength and energy are related by the expression

$$\lambda(\mathring{A}) = \frac{12.4}{E(keV)} \qquad (2.2)$$

where $1\mathring{A} = 10^{-8}$ cm. By selecting the crystal with appropriate lattice spacing and by using slits to limit the angular divergence of the beam, it is possible to construct crystal spectrometers exhibiting an energy resolution of 10 eV or less in the energy range of interest. This is more than adequate to discriminate between adjacent elements in the periodic table and eliminate almost all ambiguities in the interpretation of spectra which arise from the overlap of complex K and L x-ray spectra.

This energy resolution is achieved at a considerable loss in intensity due to the restrictive geometry necessary to produce a narrow x-ray beam. Furthermore, since only one wavelength can be reflected at a given θ setting, the spectrometer is basically a single-channel instrument and must be sequentially scanned through the range of interest. The low efficiency of the spectrometer can be compensated by using a higher incident excitation flux. Multiple crystal spectrometers are also available for simultaneous analysis of more than one element. This technique, called "wavelength-dispersive x-ray fluorescence analysis" has been in use for several decades.[1,2,3]

In the past ten years, the development of semiconductor type radiation detectors for nuclear physics applications has resulted in the availability of another technique for XRF measurements.[4] These detectors convert the energy of incident photons into ionization in the semiconductor detector material. The ionization signal is closely proportional to the photon energy, a fact which makes these devices very convenient spectrometers for XRF analysis.

Although various detectors operating on induced ionization have been available for many years, it was not until modern semiconductor detectors were developed that the energy resolution became adequate for XRF analysis. Since their introduction in the early 1960's semiconductor detector x-ray spectrometers have been continuously improved in energy resolution and counting-rate capabilities. The energy-dispersive x-ray method which has been developed around semiconductor detector spectrometers has supplanted the wavelength-dispersive method in a number of important applications. This chapter is devoted to the instrumentation associated with semiconductor detector x-ray spectrometers.

X-ray fluorescence is achieved by illuminating the sample with an appropriate source of electrons, photons, or charge particles. Fluorescence x-rays together with possible background radiation are emitted more or less isotropically from the sample. In energy-dispersive x-ray fluorescence, a semiconductor detector is placed near the sample in order to intercept and analyze a fraction of these x-rays.

A typical x-ray detector is a circular device with an active region which is 0.5 to 1.0 cm in diameter and 3 to 5 mm thick. When x-rays with energies in the range of interest for XRF are incident on semiconductor materials such as silicon or germanium they interact with the material principally by the K-shell photoelectric effect. This results in inner shell vacancies together with ejected photoelectrons whose energies are equal to that of the incident photon minus the K-shell binding energy. These vacancies de-excite either by emitting low-energy electrons or characteristic silicon or germanium x-rays which, in most cases, are then reabsorped in the detector material. The energy of the electrons produced in photoelectric interaction and in the de-excitation process is absorbed in the crystal by repeated ionizing collisions with the atoms in the lattices

which produce numerous free electrons and their associated positive holes. The number of electron-hold pairs produced is very large and there is a well defined average energy (ε) per pair. The number of free charges is therefore :

$$n = E/\varepsilon \tag{2.3}$$

where E is the initial photon energy. The semiconductor materials used in detectors are of such quality that virtually all the free carriers are collected to produce a charge signal that is accurately proportional to the initial photon energy. This pulse is then electronically amplified and shaped so as to maximize the signal amplitude relative to any random noise sources. The pulse processing system is critical in achieving the energy resolution performance required for x-ray fluorescence spectrometry.

The electronic amplifier output consists of a random time sequence of pulses with varying amplitude reflecting the emission spectrum of the sample. The amplitude of each pulse represents the energy of an x-ray, and its frequency of occurrence is proportional to the intensity of that particular type of emission.

In order to readily interpret these data, individual pulse amplitudes are digitized and a histogram of pulse amplitudes is accumulated in a multichannel analyzer. The spectrum can then be analyzed to obtain energies and intensities of x-ray lines which can then be converted to the desired analytical information. Figure 2.1 is a typical x-ray spectrum showing the K_α and K_β lines of manganese accumulated in a pulse-height analyzer.

It is important to note that the semiconductor detector simultaneously observes all x-rays incident on the detector. Therefore, a broad range of elements can simultaneously be measured with more or less uniform sensitivity. Qualitative analyses can easily be performed by a quick survey

of the spectrum, quantitative analyses require that an accurate sensitivity curve for the instrument is known.

II. SEMICONDUCTOR DETECTORS

A. General Design

The use of solid state semiconductor materials for radiation detectors results from their unique electrical properties. For any particular semiconductor there exists a temperature below which virtually no free charge carriers are present with which to sustain an electrical current when a voltage is applied. For silicon the critical temperature is well below room temperature while germanium requires lower temperatures (77°K--liquid nitrogen--is commonly used to cool both silicon and germanium spectrometers). Although the materials normally behave as insulators at this temperature, only a small amount of energy is necessary to release bound electrons which are then excited across the narrow band-gap into the conduction band where they can be collected by an applied voltage. Since the energy required to generate charge carriers is small, absorption of an energetic quantum of incident radiation results in a large number of free charges and a correspondingly large charge signal.

An important requirement of semiconductor materials for detector applications is the ability to collect all the free charge produced in photon interactions. Impurities and defects in crystals can create electrically active traps where free charges can be temporarily bound and effectively removed from the signal thus reducing its amplitude. Fortunately, with careful crystal growth and selection, it is possible to obtain materials of sufficient quality to perform suitably for detectors.

B. Detector Fabrication

Although a number of semiconductor materials has been explored for detector applications, all very high resolution spectrometers presently employ either silicon or germanium. In the case of Ge, it is possible to obtain material containing so few donors (i.e., atoms releasing electrons and therefore acting as fixed positive charges in the lattice) or acceptors (the inverse of donors) that relatively low applied voltages will deplete the material of free charge in order to form a sensitive region for radiation detection. Such high-purity germanium detectors are currently available although their use in x-ray applications is limited for reasons to be discussed. They are applied mainly to the detection of high-energy x-rays and γ-rays where the higher atomic number and correspondingly greater photoelectric cross sections of Ge contribute to increased absorption efficiency.

Most semiconductor detector x-ray spectrometers used in x-ray fluorescence employ lithium-drifted Si detectors (Si(Li)). For that reason they will be described here in more detail than other types of devices; although, most of the general ideas regarding their properties will be applicable to others. Figure 2.2 shows a cross section of Si(Li) detector. Typical dimensions might be 2 cm total wafer diameter and 3 to 5 mm thickness. The active area is defined by the mesa structure in the middle and is typically 5 to 10 mm in diameter. The bulk of the detector volume constitutes the active region where events are detected. Since Si is not available with sufficiently low doping levels due to purification problems, it is necessary to compensate the acceptor sites in the detector volume. Starting with p-type material (i.e., mainly acceptor-doped), it is possible to drift lithium donor atoms into the volume under an applied field in such a way that they

perfectly compensate the number of acceptors. The number of effective free charge carriers is thereby reduced almost to zero, and the application of relatively low voltages will deplete sufficient thickness of material (several mm) to serve as a detector.

To deplete the active volume and provide the electric field required to collect the radiation-induced free carriers (holes and electrons), it is necessary to apply a voltage of a few hundred volts across the detector bulk. For the detector to withstand this voltage without injecting charge from the contacts, opposite faces of the detector are heavily doped with p- and n-type impurities. The n-type contact is then biased at a positive voltage with respect to the p-type. Since the strongly doped contacts contain few minority carriers, virtually no current can be injected from the contacts into the detector volume. Such a detector is referred to as a p-i-n structure where i refers to "intrinsic" or carrier free region and p and n refer to the two contacts.

C. Signals, Noise, and Resolution

Since the signal of interest consists of a pulse of charge collected across the detector, it is obvious that the accuracy of measurement of the signal is affected by spurious charges collected at the electrodes or otherwise introduced into the electronic system. One important consequence of this is the necesssity to cool detectors to reduce the production of free carriers by thermal vibrations in the lattice. Since silicon and germanium have finite energy gaps across which charges can be excited, a number of free charge carriers are normally available to sustain a current with an applied voltage. By reducing the temperature, this leakage current is drastically reduced. For high-resolution

x-ray spectrometers, detectors are normally operated in vacuum cryostats at temperatures approaching liquid nitrogen (77°K).

Although cooling reduces the detector leakage, it is unavoidable that some noise sources remain not only in the detector but also arising from random fluctuations in currents in the later amplifying stages. Such noise sets a fundamental limit to the energy resolution which can be achieved. The electronic signal processing is designed to reduce this to a minimum; modern spectrometers are characterized by electronic contributions to resolution in the range of 60 to 100 eV full width at half maximum (FWHM).

The total energy resolution when observing x-rays is a combination of this electronic noise and a contribution due to statistical fluctuations in the ionization process in the detector. The total number of hole electron pairs produced by a particle of energy E has previously been defined by Eq. 2.3. Since the formation of these charge pairs is a statistical process, there is a deviation in this number which can be expressed as

$$E_{FWHM} = 2.35\sqrt{E\ \varepsilon\ F} \qquad (2.4)$$

This equation is similar to that for a Poisson distributed variable with the exception of the factor F. This so-called Fano factor takes into account the fact that the interaction processes which produce free charge in the detector are not completely statistically independent. Measured values for F in Ge or Si range form 0.08 to 0.13. Combining this with a value of ε of 2.96 for germanium and 3.7 for silicon, the contribution due to charge-production statistics to the total resolution is approximately 100 eV for germanium and 120 eV for silicon.

The energy resolution of semiconductor spectrometers is the quadrature sum of electronic noise and statistical spread. The full width at half maximum ΔE, can be expressed as

$$\Delta E = \sqrt{E_N^2 + E_D^2} \tag{2.5}$$

where E_N is the FWHM contribution of electronic noise and E_D is due to charge-production statistics. Figure 2.3 is a plot of this relationship for a variety of cases.

D. Efficiency of Semiconductor Detectors

The total efficiency of a semiconductor detector x-ray spectrometer is determined by the product of geometric efficiency and intrinsic detector response. The geometric efficiency is a solid angle subtended by the detector at the sample to detector distance. For typical x-ray fluorescence spectrometer applications, detector/sample distances of 2 to 10 cm are employed, corresponding to geometric efficiencies in the range of 1% to 0.04%. The intrinsic efficiency of a detector is defined as the probability that an x-ray incident on the sensitive region of the detector will be absorbed and produce a signal. Figure 2.4 shows plots of the intrinsic efficiencies of typical Si(Li) and Ge detectors as a function of photon energy. The efficiency at low energies is limited by absorption in the entry window of the detector and in any materials (including air) between sample and detector. A typical entrance window on a Si(Li) detector consists of a 0.2 μm dead layer on the p^+ contact side. The cryostat entry window is typically a pure beryllium foil 25 μm thick. The remaining x-ray path may be either air, vacuum or helium depending on the application. At the high-energy end of the curve, the efficiency is proportional

to $(1-e^{-\mu\rho x})$ where $\mu\rho$ is the photoelectric cross section in cm^{-1} and x is the detector thickness.

E. Background

In the foregoing discussion, it has been assumed that the spectral response of a detector to monoenergetic x-rays is a single Gaussian-shaped peak with resolution determine by Eq. 2.5. However, several mechanisms contribute to a more complex response.

1. X-ray escape peak

The primary interaction of x-rays with the detector material results in the photoelectric ionization of an inner shell. The resulting vacancy often de-excites by emitting a characteristic x-ray of the material. The K_α energy for silicon is 1.74 keV while for germanium it is 9.8 keV. When photoelectric events occur deep within the detector, the characteristic detector material x-rays are reabsorbed and contribute to the full-energy signal. However, for events which occur near the surface, there is a significant probability that the characteristic radiations escapes and a corresponding amount of energy is lost from the signal. This results in "escape" peaks at energies 1.74 keV (Si) or 9.8 keV (Ge) below the full energy peaks. The magnitude of these peaks is proportional to the fluorescence yield for the vacancies in the detector material and depends upon the absorption depth of the incident radiation. The peaks are most prominent when the incident photon energy is just greater than the absorption edge energy. Figure 2.5 is a spectrum of zirconium x-rays detected by a Ge detector showing the K_α and K_β escape peaks. Since the fluorescence yield for the Ge K-shell is large (ω_K = 0.5), the magnitudes of the escape peaks are much

larger than for silicon where ω_K = .06. The enhanced escape probability and its adverse effect on the interpretation of complex spectra complicates the interpretation of x-ray fluorescence spectra obtained with Ge detectors.

2. Continuum background

All x-ray fluorescence spectra exhibit continuous background distributions which span the energy region of interest in XRF analysis. Since fluctuations in this background can hide real peaks, the identification and reduction of the effects which produce background are important objectives for improving analytical sensitivity. The complete process whereby the photon energy is converted into a charge signal involves a number of intermediate steps in which energetic electrons, holes, and photons are produced in the crystal. Any escape of radiation from the active volume, results in a background of partial amplitude pulses. In most applications these fundamental background processes do not appear to seriously limit the use of the detectors.

There is one source of continuous background arising from detector artifacts which is potentially serious but can be reduced by careful experimental design. This results from incomplete collection of the charge due to irregularities in the electrostatic field lines within the detectors.[5] Figure 2.6 shows a common type of detector geometry employed for x-ray spectrometers. Where the intrinsic material reached the surface of the device, it usually behaves as a lightly n-doped surface layer and the resulting internal electric field lines are distorted as shown. Since charge collection occurs along these field lines, some of the charge is collected via the surface layer. Once charge reaches the surface,

it becomes trapped for sufficiently long times that it no longer contributes to the normal input signal. These events produce partial amplitude signals. In some detectors as many as 40% of the signals produced by 20 keV photons are degraded into a low-energy continuous background distribution. This effect can be reduced by the use of external collimation to restrict the effective area of the detector to a small central region[6] or by using internal electrostatic collimation in the form of a guard-ring detector as shown in Fig. 2.6. Here a larger area device is fabricated but the signal is extracted only from an electrically isolated central portion. This method, together with circuitry which rejects pulses where charge is shared between the central and outer detector regions, reduces the background due to incomplete charge collection resulting in substantial improvement in the detectability of peaks in complex spectra. This technique is particularily important in the case of photon-excited x-ray fluorescence where the scattered photons occur in the high-energy portion of the spectrum. A continuous distribution of degraded pulses resulting from these events would seriously limit the detectability for this type of measurement.

III. SIGNAL PROCESSING ELECTRONICS

A. Input Circuit-Preamplifier

1. Choice of field-effect transistor

The signal processing electronics that amplifies and processes the weak detector signals is critically important in an x-ray spectrometer. The electronics is generally comprised of a preamplifier, placed in very close proximity to the detector, and a main amplifier which may be located some distance from the detector

and its cryostat. The preamplifier usually contains a front-end amplifying element and associated components which are mounted near the detector inside the cryostat, while the remaining preamplifier components are placed as close as possible outside the vacuum wall of the cryostat. Modern high-resolution x-ray spectrometers employ selected field-effect transistors (FETs) which exhibit very low noise when operated at an optimum temperature in the region of 140°K. Since the detector is operated near 77°K to minimize its leakage current, the FET temperature must be raised slightly by providing a suitable heating/thermal resistance arrangement.

Selection of suitable low-noise FETs is a time consuming process, since very few samples of standard commercial FETs exhibit the required behavior at low temperatures. The inferior performance of most FETs is generally attributed to the presence of uncontrolled impurities which provide traps in the active region of the device where generation and recombination of holes and electrons can occur. Fluctuations in this process, as observed in the frequency range set by the amplifier bandwidth, are temperature-dependent and they contribute to a degradation in the energy resolution of the system.

Choice of a suitable FET is also based on matching the device to the detector capacitance. Input signals consist of charge produced in the sensitive region of the detector which flows in the external circuit as it is collected. Figure 2.7 shows the basic input circuit factors which contribute to determining the energy resolution of the spectrometer. The following parameters are important:

Detector signal--Q

Detector capacitance--C_D

FET input circuit capacitance--C_{in}

Detector leakage current--i_D

FET gate leakage current--i_G

FET channel noise represented by a series voltage noise source e_n

The value of e_n is given by:

$$\overline{e_n^2} = 4KR_F T\Delta f \tag{2.6}$$

where K is Boltman's constant

T is the temperature (°K)

Δf is the bandwidth of the system

and R_F is the FET noise resistance given approximately by

$$R_F = 1/g \tag{2.7}$$

where g is the transconductance of the FET. In the design of an FET, the transconductance of g and the FET capacitance C_{in} are linked and for practical purposes the ratio g/C_{in} can be regarded as constant.

As far as the FET channel noise is concerned, it can be represented by the generator e_n and, for signal/noise calculations, it is to be compared with the voltage signal $Q/(C_D + C_{in})$. The signal/noise ratio (for this noise source alone) is clearly proportional to $Qg^{\frac{1}{2}}/(C_D + C_{in})$ and therefore proportional to $QC_{in}^{\frac{1}{2}}/(C_D + C_{in})$. It is easy to show that his expression has its maximum value when $C_D = C_{in}$ and therefore that the FET should ideally be chosen to satisfy this condition. In this case, the signal/noise ratio will be proportional to $Q/C_D^{\frac{1}{2}}$. Clearly, the best resolution is obtained

by using a small area detector thereby minimizing C_D; however, the efficiency for detecting x-rays must also be considered, so, for typical x-ray fluorescence systems, a compromise of a 0.5 to 1 cm diameter detector is usually employed. This results in a detector capacitance ~1 pF. While the ideal FET, by these arguments, would be one having a similar capacitance, practical considerations have resulted in the use of FETs of the 2N4416 generic class having $C_{in} \simeq 3$ pF and g ~5 mA/V.

It is obvious from Fig. 2.7 that e_n is not the only noise source, since fluctuations occur in both the detector and FET gate leakage currents. Furthermore, any additional parallel input components, (such as a biasing resistor), would contribute noise. These parallel sources produce noise which, when expressed as an input voltage, is clearly proportional to $1/(C_{in} + C_D)$ as is the signal. Consequently, from the point of view of these noise sources, as distinct from the FET channel noise represented by e_n, the signal/noise is independent of the total circuit input capacitance $(C_{in} + C_D)$.

2. Charge-sensitive method

The most obvious type of preamplifier would be a conventional voltage-sensitive amplifier. However, such a system would produce output voltage signals which would depend on the detector capacitance. This might result in rather serious drifts in signal amplitudes, since the surface channels on detectors change with time, contributing small changes in detector capacitance. Consequently, x-ray spectrometers all employ a feedback operational amplifier with a capacitive feedback element as shown in Fig. 2.8, to produce an output signal whose amplitude is proportional to the charge flowing

through the detector. Detector capacitance changes (within limits), then produces virtually no change in the output signal (although they do affect signal/noise and therefore resolution). The output signal V_o from the charge-sensitive stage is given by;

$$V_o = Q/C_F \tag{2.8}$$

where C_F is the feedback capacity value.

3. Pulsed-light feedback

The simple operational amplifier integrator of Fig. 2.8 would integrate the charge flowing in the detector resulting both from leakage current and radiation-produced ionization in the detector. Therefore, the output would drift in a positive direction with time and would soon saturate. Consequently, a method must be provided to discharge C_F and thereby maintain the preamplifier in its linear range. For many years, the method commonly used employed a high-valued resistor across C_F to provide a discharge path. This is far from ideal, since the resistor acts as a noise source and adds capacitance in the input circuit. Furthermore, high-valued resistors do not behave as pure resistors and their behavior causes difficulties in achieving good resolution at high-counting rates.

Most modern x-ray spectrometers employ a pulsed method to discharge C_F periodically. The pulsing may follow each event or, more commonly, may be initiated when the preamplifier output reaches an upper dc level where a discriminator fires to start the charge restoration process. Charge restoration ends when the output falls to a predefined lower level. The pulse processing system is made insensitive during this reset time, so no inputs are processed during the few microseconds while C_F is being discharged. Since

no dc discharge current is present when signals are being processed, no noise is produced by the discharge process. This is in contrast to the resistor and "dynamic charge restoration" methods.

The most common pulsed restoration technique uses a pulsed light-emitting diode (LED) to cause substantial leakage current to flow in the FET drain to gate junction.[6] This is known as the pulsed-light or pulsed-opto feedback method. Since this is in very common use, we will describe it in more detail with the aid of Fig. 2.9.

The detector is connected to the FET gate with negative detector bias applied to the p contact. Leakage current and photon-induced charge is integrated by the feedback capacitor C_F causing the output to rise in voltage. When the output level crosses the upper trigger threshold of the Schmitt trigger circuit, the LED is turned on (after a slight delay). Light from the LED is directed onto the FET causing a substantial photocurrent to flow from drain to gate of the FET. This current, integrated by C_F, causes the output voltage to fall rapidly until it reaches the lower trigger threshold of the Schmitt trigger circuit. At this point, the light is immediately turned off. The Schmitt circuit is designed for a 2V difference between its two trigger levels and the discharge of C_F(~0.1 - 0.2 pF), through this voltage requires only a few microseconds. In normal use, the discharge cycle is only repeated every 10 to 100 ms so the loss of counts during the discharge is almost negligible. However, during the reset period, the preamplifier provides a blanking waveform which is used to inhibit baseline restoration at the output of the main amplifier during this period.

B. Amplifier Requirements

1. Gain, linearity

Essentially, the preamplifier provides a very low impedance input to match the detector and a low output impedance to drive the cable to the main amplifier. It may also contain a certain amount of gain to increase signals and thereby to reduce the effect of any extraneous electrical noise picked up on this cable. Most of the gain in the system is provided by the main amplifier. The overall system gain requirement is easy to calculate. Since the detector is a source of signals consisting of a few hundred electrons (e.g., ~300 for a 1 keV x-ray), and its capacitance is about 1 pF, typical output voltages for the charge integrator are in the range of 50 μV. An adequate output level from the main amplifier to the digital processing system is typically a few volts. Consequently, in this crude picture, the requirement is for a gain in the range of 10^5.

For many purposes, a rather precise linearity between input and output signal must be maintained, since non-linearity of response would result in complications in interpreting spectra, particularly when computer processing is used. Generally speaking, the output must not deviate by more than 1% at any amplitude compared with its predicted value on the basis of a true linear response.

Another essential amplifier characteristic is the ability to adequately handle large overload pulses, (i.e., to recover from the overload quickly and without producing spurious output signals). This requirement is particularly important in pulsed reset systems, since a very large signal of the opposite polarity from normal signals results from the discharge of the feedback capacitor in the preamplifier.

2. Pulse shaping and its effect on resolution

The main amplifier also performs a very critical operation which is of great importance in determining the energy resolution of x-ray spectrometers. This operation consists of shaping the signal pulse to permit the best possible measurement of each signal amplitude despite the effects of noise of various kinds and of the possible interference of other (earlier) signal pulse residues. The topic of optimum signal processing is much to extensive for this short treatment of x-ray systems, so we will restrict this discussion to some rather basic features of the subject. The simplest picture of the pulse-shaping process is to regard it as a method of restricting the system bandwidth to a minimum value consistent with retaining the signal and thereby cutting out noise in the frequency regions not required to process the signal. This simple picture implies a low-frequency limit--therefore a differentiator--and a high-frequency limit--therefore an integrator. The existence of an integrator and differentiator implies that the shaping system converts the input signal, which is a voltage step, (see Fig. 2.8) into a pulse of limited rise time and duration. A short duration pulse is also essential to present interference between successive signal pulses, but the optimization of resolution generally requires longer pulse widths than is desirable from the point of view of avoiding interpulse interference. Therefore, some compromise must be made between resolution and performance at high-counting rates.

To simplify the understanding of pulse-shaping techniques, we will define a parameter that we term "measurement time (T_m)."

In principle, this can be any characteristic time of the amplifier output pulse shape; for convenience, we will use the pulse width as measured at the points on the rising and falling edges corresponding to 5% of the full pulse amplitude. Figure 2.10 shows some characteristic pulse shapes and the relationships that exist between our defined measurement time (T_m) and other time parameters. Most pulse shaping circuits are passive--that is they contain circuit elements which are fixed and do not change with time. The RC integrator, differentiator of Fig. 2.10(1), is the simplest example. The long tail on this pulse is detrimental to the performance of a system at high-counting rates, so this type of shaping is rarely employed. The use of multiple RC integrators, as in Fig. 2.10(2), results in more symmetrical pulse shapes. As the number of integrators is increased, a Gaussian pulse shape is approached. The symmetry of these pulse shapes leads to a good compromise between energy resolution and high-rate performance. Consequently, such pulse shapes (with >4 integrators), or slightly modified versions, are very commonly employed in x-ray spectrometers. Somewhat better performance can be achieved by some so-called active pulse shapes in which the values of components are switched in time, syncronous with the signal. A simple example is the gated-integrator shown in Fig. 2.10(3), but more complex systems are slowly coming into use.

While the various types of pulse shapes achieve somewhat different energy resolutions and rate performance, once a type of shaper is selected, the characteristic times of the output pulse, including T_m, must be chosen. Since T_m largely controls both energy resolution at low-counting rates, and its degradation at high rates, choice of the optimum value of T_m for a given application is

critically important. Many systems permit the user to adjust the measurement time to suit the application. The effect of measurement time on the electronic component of energy resolution is illustrated in Fig. 2.11. The parameter T_o is the peaking time for a Gaussian shaped pulsed, $T_m \approx 2\ T_o$. As T_m is increased from a small time, we see that the resolution improves initially ($Res^2 \propto 1/T_m$), passes through an optimum value and then starts to rise ($Res^2 \propto T_m$). The short time part of the curve is dominated by channel noise in the FET (e_n in Fig. 2.7), while the long time behavior results from the leakage noise (i.e., fluctuations in i_g and i_D of Fig. 2.7). In the context of this discussion, "energy resolution" refers solely to the electronic noise contribution. Detector charge production statistics, as discussed in Section II(C), are not included. The depth of the valley in the curve in the region of the optimum value of T_m is determined partly by the absolute magnitude of these noise terms and also by miscellaneous noise sources (generally called 1/f noise--including insulators, surface noise in the FET detector, etc.), which produces a flat noise distribution independent of T_m.

Improvements in energy resolution over the past 10 years have largely been the result of achieving reduced 1/f noise, decreasing the leakage currents and their associated noise and of the use of pulsed light feedback which removes all noise due to currents discharging C_f in Fig. 2.8. These improvements have all resulted in an increase in the optimum measurement time T_m, from the point of view of resolution. The use of measurement times as long as 100 μs has made the problem of maintaining performance at high-counting rates more difficult. Improvement of the short measurement time

part of the curves of Fig. 2.11 depends on the possible availability of FETs with much better g/C_{in} ratios than present day devices. While some progress is being made in this direction, any immediate change in the situation cannot be anticipated.

C. System Considerations

The previous discussion can best be focussed by studying a complete x-ray spectrometer electronic system as shown in Fig. 2.12. While other systems differ in many details, the general features must be provided in any modern spectrometer.

Signals from the preamplifier are fed to the input of this unit. The main linear amplifier block performs the functions of differentiation, amplification and multiple integration to produce approximately Gaussian shaped pulses at its output. This output is then fed to a baseline restorer which accurately defines the baseline levels of the signals; from this point through to the analog digital converter, which follows this unit, dc connections are used and the baseline established by the restorer applies to all pulse amplitude measurements. Fluctuations in the baseline at high-counting rates will seriously degrade the energy resolution, so the restorer is designed to reduce such fluctuations to a minimum consistent with not significantly altering the basic signal pulse shape. Since the restorer normally clamps on negative voltage excursions, the very large negative signals which occur whenever the preamplifier resets would produce very serious effects on the baseline. Consequently, the clamping action of the restorer is inhibited during the preamplifier reset pulses and for a short time thereafter.

In addition to the main signal path, the preamplifier signal is differentiated to produce short signals which are amplified by the fast

amplifier. A fast discriminator included in this block provides signals corresponding to the start of the Gaussian-shaped signals produced by the main amplifier channel. These fast signals are available for use externally (e.g., for timing purposes), but are also used internally for pile-up rejection. The pile-up rejection circuit inspects to find whenever the interval between two fast pulses is sufficiently short that two pulses will interfere with each other in the slow pulse-height measuring channel. If so, one or both, (depending on the actual case), of the pulses are removed by preventing the signal discriminator from firing, thereby stopping transmission of signals through the stretcher to the output.

Signals from the baseline restorer output feed a stretcher circuit and, if they exceed a lower level set by the discriminator and satisfy pile-up criteria (i.e., they are not contaminated by other pulses), they are stretched at their peak amplitude. The differential linear gate is then used to generate a rectangular signal output pulse equal in amplitude to the signal peak height minus the discriminator bias level. Only that part of signals exceeding the bias level is passed on to the output amplifier, where signals are amplified to conform to the signal amplitude range of the pulse-height analyzer.

Dead time corrections must be applied in all quantitative applications of x-ray spectrometers. This is done by automatically adjusting the counting time to extend it by a factor sufficient to correct for those signal pulses lost due to system dead time. This is usually accomplished by counting a stream of accurately timed clock pulses gated by a dead time waveform generated by the pulse processing system. The resulting output clock pulses are a measure of the "live time" of the spectrometer. The dead time waveform must accurately represent

losses due to the pile-up rejector process as well as any dead time in the pulse-height analyzer.

D. Pulsed-Excitation Technique

When using conventional continuous excitation sources and heavy samples, a condition where very high event rates occur in a detector, the pile-up rejector circuit of Fig. 2.11 may reject almost all the pulses so very few reach the analyzer. The relationship between the system output rate and input rate for a certain value of the pile-up inspection time is shown in Fig. 2.13. It is seen that the output rate follows the input rate at low input rates, then falls for very high input rates. The peak output rate occurs at an input rate equal to 1/(Pile-up Inspect Time) and is 1/e times the input rate at this point. As discussed above, the optimum resolution in x-ray systems occurs at long measurement times and pile-up inspection times of 50 μs or more are quite common. If we assume 50 μs, the output rate is limited to about 7 kc/s (i.e., 20/e).

A better output rate can be achieved if a pulsed excitation source, (such as a pulsed x-ray tube or a pulsed ion beam) is used in place of the dc excitation.[7] In a pulsed system, the beam is turned on at high level and turned off as quickly as possible when a signal is detected in the system (for example, by the fast discriminator of Fig. 2.12). The excitation source is turned on again when the signal has been processed. In such a scheme, each pulse can be processed with almost no chance of pile-up since the excitation source is turned off during the pulse processing time. A small chance does exist of a second pulse arriving in the small time interval between the sensing of a signal and the excitation disappearing (an interval typically of only ~100 ns). the input/output rate behavior of a pulsed system is shown in the second

curve of Fig. 2.13. It is seen that the input curves track very well until the rate reaches 1/(Pulse Processing Time). Obviously, this rate cannot be exceeded under any circumstances, but this output rate is almost a factor of three greater than can be achieved in a spectrometer using dc excitation.

The advantages of the pulsed excitation method are not achieved without some cost in complexity. It is necessary that the excitation source intensity should, as far as possible, be automatically adjusted for the system to operate near the peak of the curve of Fig. 2.13. For heavy samples this means reducing the source intensity while light samples require maximum power operation of the source. Therefore, the excitation intensity is not constant and it cannot be used as a reference for comparison of different samples that are counted for a fixed live time. Instead, the integral of the intensity must be measured and counting carried out for a fixed value of this integral. If a pulsed x-ray tube is used as the excitation source, the total charge through the tube is a good measure of the integral of the intensity. The complexity of these techniques prohibits their use except in situations where very large-scale analyses of samples are required and the maximum throughput is essential. The method has been applied and is almost essential to handle the volume of samples generated in large-scale studies.

IV. DIGITAL PROCESSING

The output of the electronic system shown in Fig. 2.10 consists of a sequence of pulses of varying amplitude which reflect the energy distribution of photons in the fluorescence spectrum. In order to display and interpret this information, the amplitude of each pulse is measured, converted to a digital number, and stored in histogram fashion in a suitable

memory array. The histogram pulse height spectrum is then available for subsequent examination and interpretation.

There are a number of commercial multichannel analyzer manufacturers who make instruments suitable for this operation. For typical x-ray fluorescence applications, a total of 1,024 channels is used to encode pulses over an energy range of 30 keV or less. This implies that a 200 eV wide Gaussian peak would be represented by seven channels above the half-maximum point of the distribution. This is more than adequate for most applications.

Commercial pulse height analyzers often include computerized facilities for locating x-ray peaks, calculating intensities, and applying calibration data to the fluorescent intensities. There are a number of methods employed for spectral analysis and for correcting the intensities for interferences from other x-ray lines and for x-ray absorption effects. The choice of method depends to a large extent on the nature of the sample studied and the degree of automation desired. More complete discussions of spectral analysis are available in the literature.[8]

REFERENCES

2.1 Jenkins, R., An Introduction to X-ray Spectrometry, Heyden and Son, New York, 1974.

2.2 Birks, L. S., X-ray Spectrochemical Analysis, 2nd ed., Interscience Publishers, New York, 1969.

2.3 Leibhafsky, H. A., Pfeiffer, H. G., Winslow, E. H., and Zemany, P. D., X-ray, Electrons, and Analytical Chemistry, Wiley-Interscience, New York, 1972.

2.4 Goulding, F. S. and Stone Y., Semiconductor Radiation Detectors, Science, Vol. 170, 280-289, 1970.

2.5 Goulding, F. S., Jaklevic, J. M., Jarrett, B. V. and Landis, D. A. Detector Background and Sensitivity of X-ray Fluorescence Spectrometers, Advances in X-ray Analysis, Vol. 15, 470-482, Plenum Press, New York, 1972.

2.6 Landis, D. A. , Goulding, F. S., Pehl, R. H. and Walton, J. T., Pulsed Feedback Techniques for Semiconductor Detector Radiation Spectrometers, IEEE Trans. Nucl. Sci., NS-18, No. 1, 115-124, 1971.

2.7 Jaklevic, J. M. and Goulding, F. S., Semiconductor Detector X-ray Fluorescence Spectrometry Applied to Environmental and Biological Analysis, IEEE Trans. Nucl. Sci., NS-19, No. 3, 384-391, 1972.

2.8 Jaklevic, J. M., Loo, B. W. and Goulding, F. S., X-Ray Fluorescence Analysis Of Environmental Samples, Ann Arbor Science, Ann Arbor, Michigan 1977.

FIGURE CAPTIONS

Figure 2.1 Typical x-ray spectrum showing Mn, K_α and K_β x-rays. The pulser peak is electronically generated and represent the noise contribu- to total resolution.

Figure 2.2 Cross section of a typical lithium-drifted silicon detector.

Figure 2.3 Resolution as a function of energy for several choices of parameters. Typical values for x-ray detectors might be 100 eV electronic noise with F = 0.12.

Figure 2.4 Efficiency vs energy for a 3 mm thick silicon detector and a 5 mm germanium detector. The low-energy limit to efficiency is determined by window absorption.

Figure 2.5 Spectrum of zirconium K_α and K_β x-rays as measured with a germanium detector showing the system peaks due to radiation escape from the detector.

Figure 2.6 Field distribution within Si(Li) detectors.

a) Typical detector exhibiting field distortions due to surface channels

b) Guard-ring detector showing a sensitive region defined by internal field lines.

Figure 2.7 Noise sources in a semiconductor spectrometer.

Figure 2.8 Charge sensitive preamplifier.

Figure 2.9 Details of a pulsed-light feedback preamplifier. The light-emitting diode (LED) is turned on when the output of the charge integrator exceeds the level set by the Schmitt discriminator.

Figure 2.10 Some common pulse shapes used in x-ray spectrometer amplifiers.

a) RC differentiator--RC integrator

b) RC differentiator--multiple RC integrator

c) Gated integrator

Figure 2.11 The effect of measurement time on resolution. T_o is the peaking time for a symmetric Gaussian shape $T_m \approx 2\ T_o$. The ordinate is given either in the number of hole-electron pairs ($\overline{N^2}$) or in equivalent eV.

Figure 2.12 A complete x-ray spectrometer electronic system including base-line restorer and pile-up rejector.

Figure 2.13 Output-counting rate verses input-counting rate. T_d is the system dead time and is normally slightly greater than the measurement time discussed in the text.

a) Conventional dc source

b) Pulsed-excitation system.

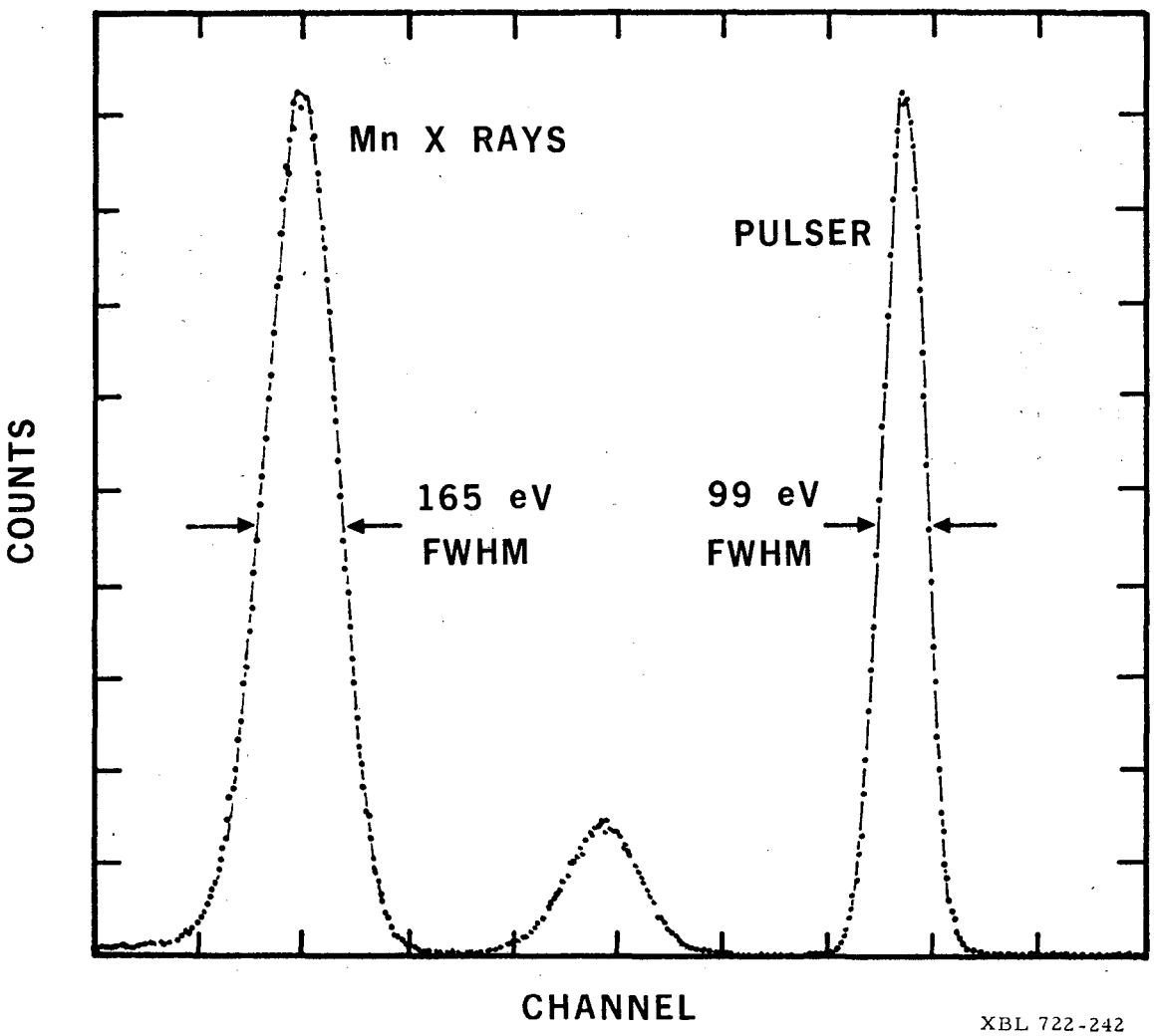
Mn X RAYS
PULSER
165 eV
FWHM
99 eV
FWHM
COUNTS
CHANNEL
XBL 722-242

Fig. 2.1

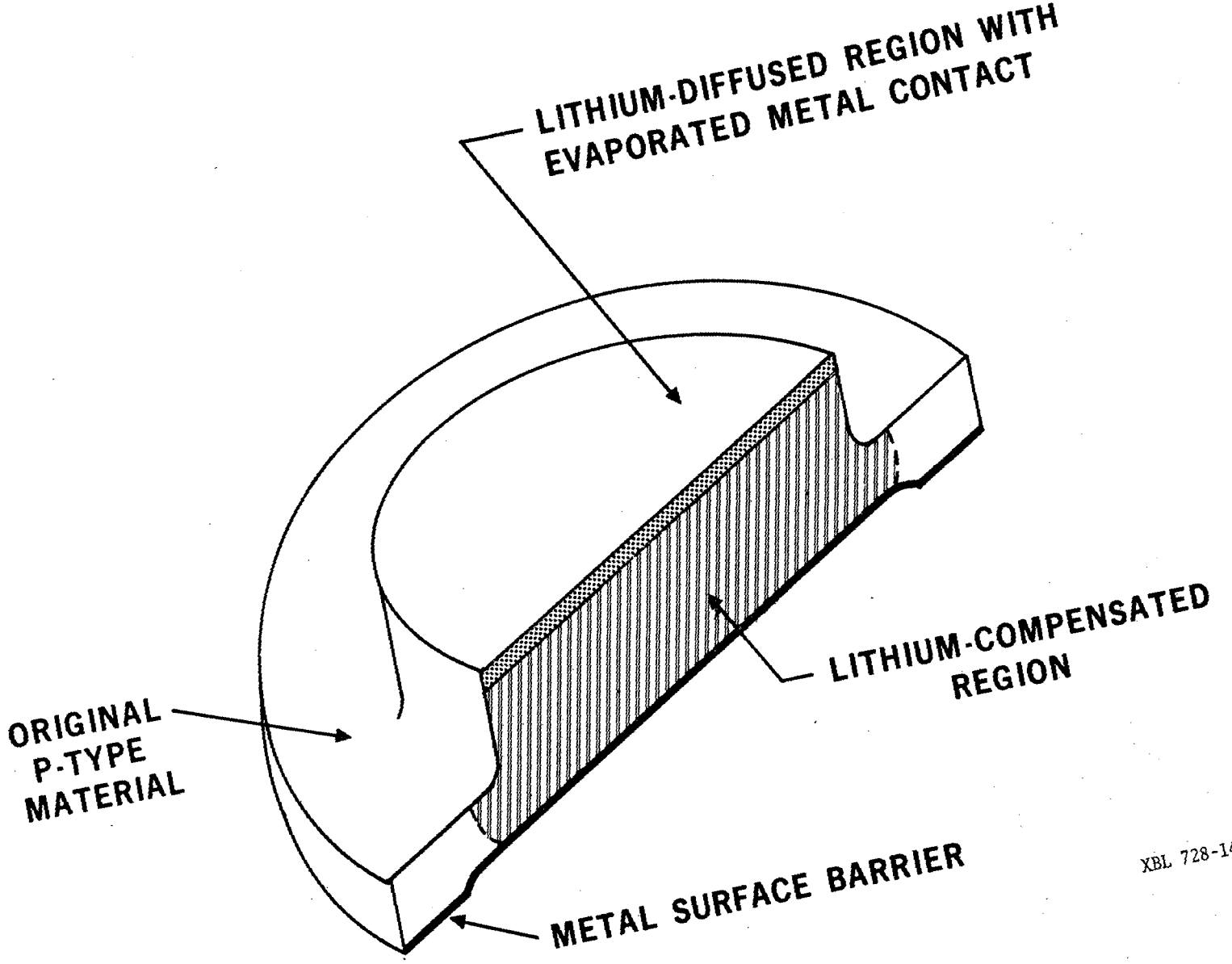

XBL 728-1492

Fig. 2.2

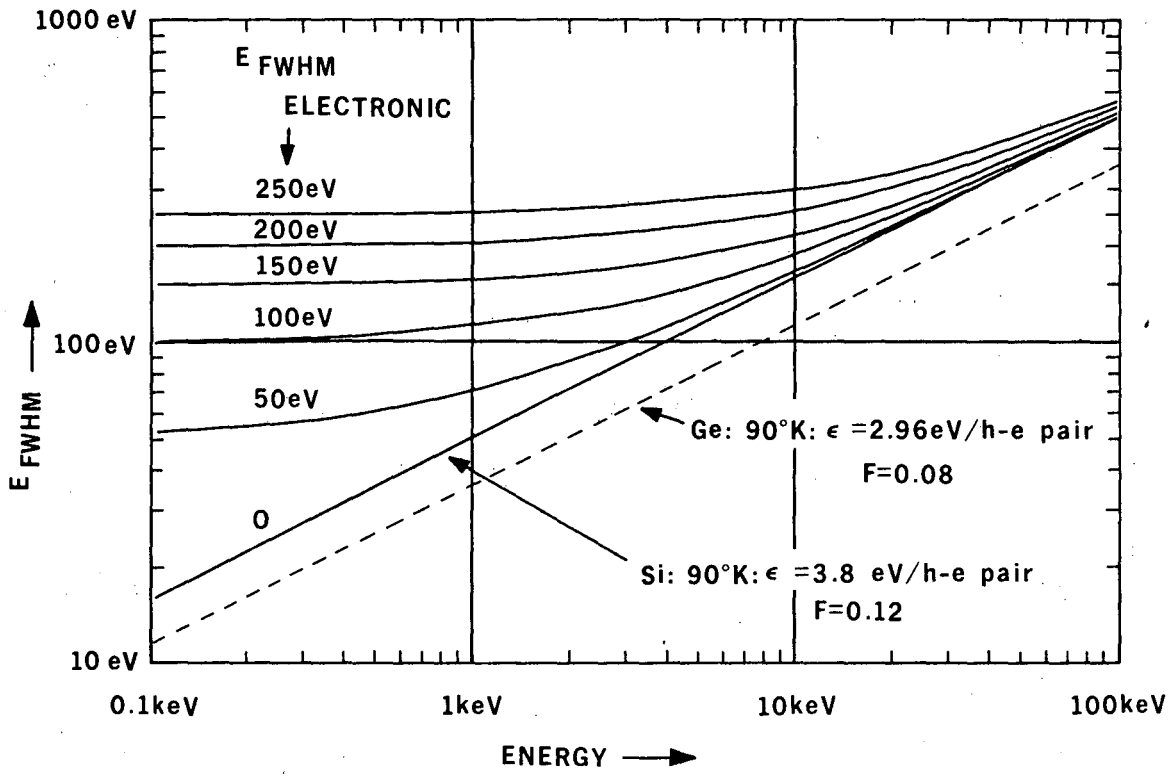

XBL 724-788

Fig. 2.3

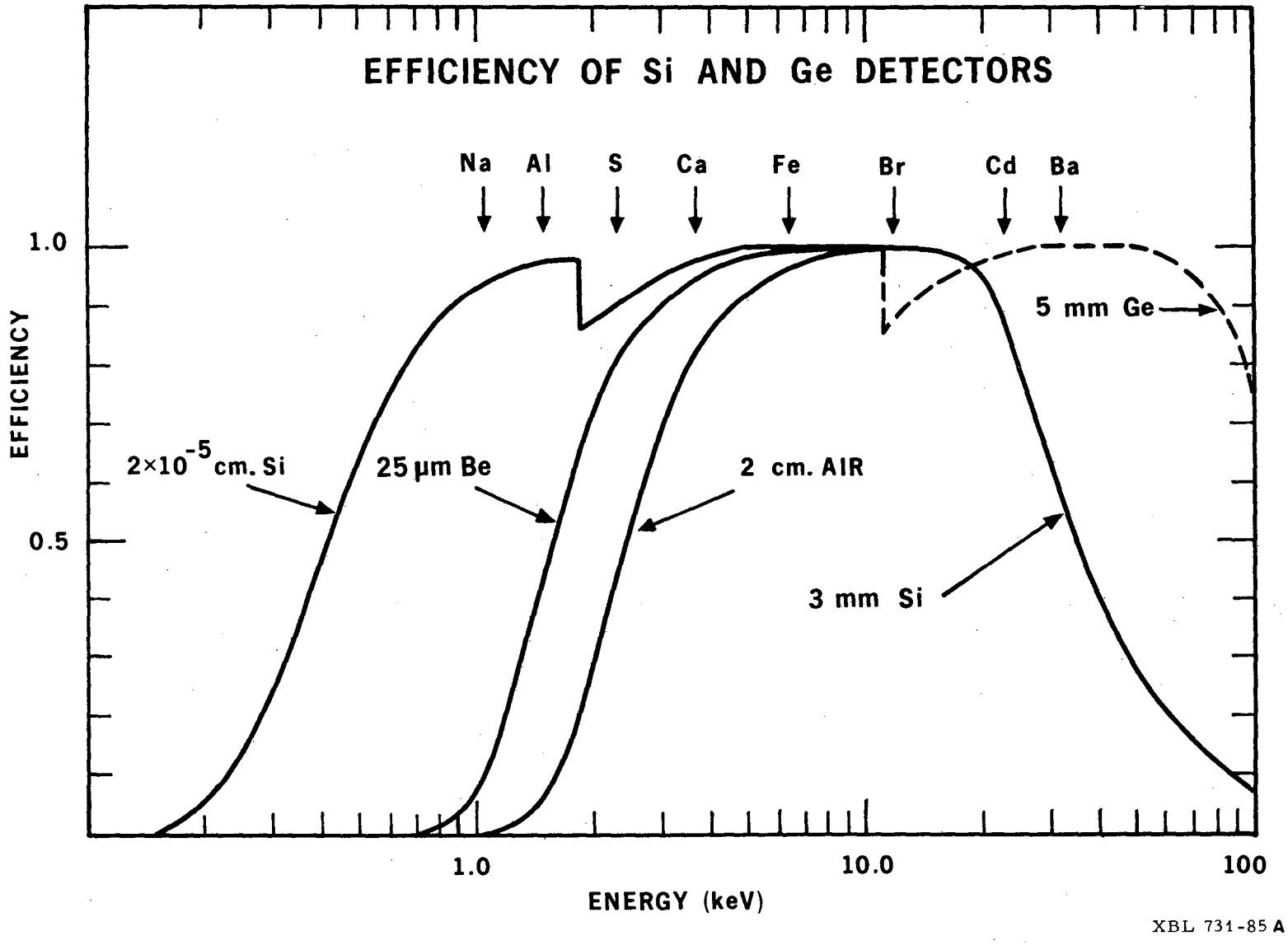
EFFICIENCY OF Si AND Ge DETECTORS
Na
Al
S
Ca
Fe
Br
Cd
Ba
1.0
0.5
EFFICIENCY
5 mm Ge
2×10-5 cm. Si
25 µm Be
2 cm. AIR
3 mm Si
1.0
10.0
100
ENERGY (keV)
XBL 731-85 A

Fig. 2.4

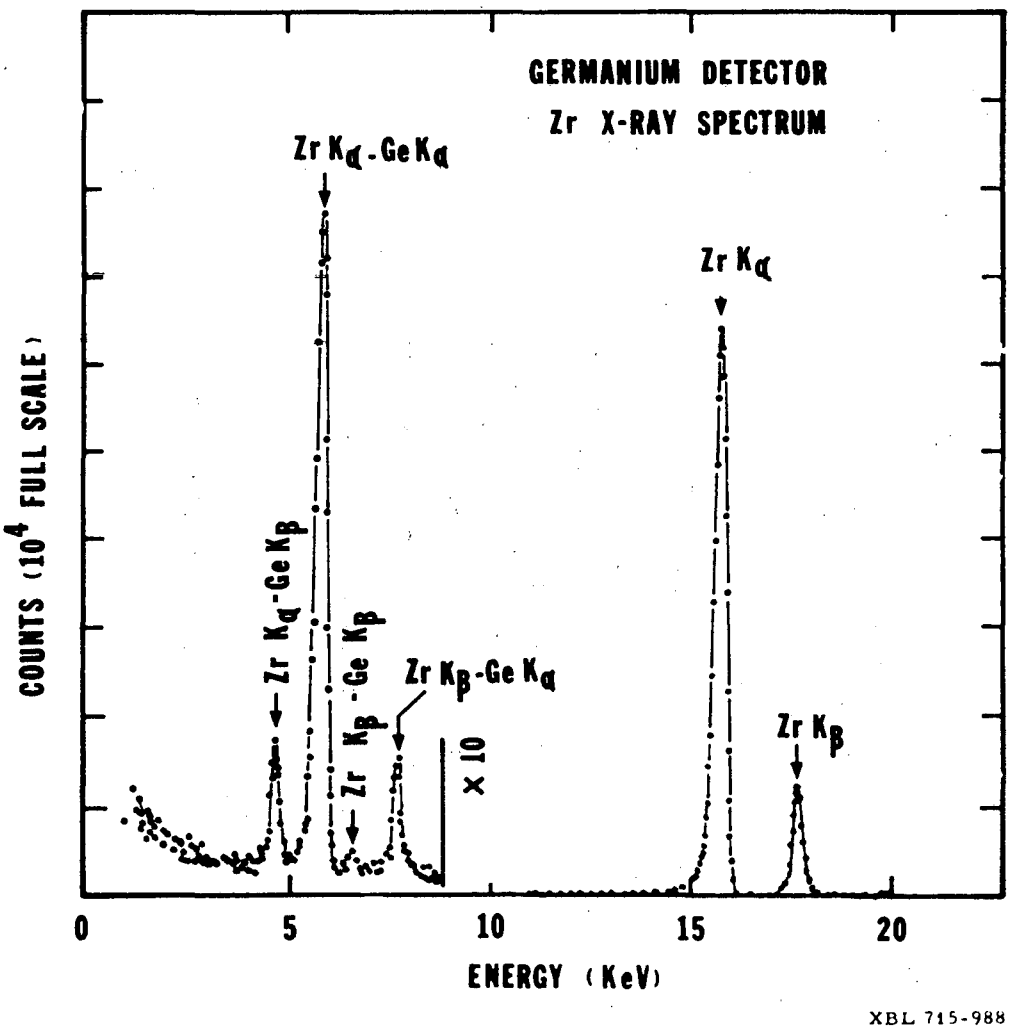
GERMANIUM DETECTOR
Zr X-RAY SPECTRUM
Zr Kα - Ge Kα
Zr Kα
Zr Kα - Ge Kβ
Zr Kβ - Ge Kα
Zr Kβ - Ge Kβ
Zr Kβ
× 10
COUNTS (10⁴ FULL SCALE)
0
5
10
15
20
ENERGY (KeV)
XBL 715-988

Fig. 2.5

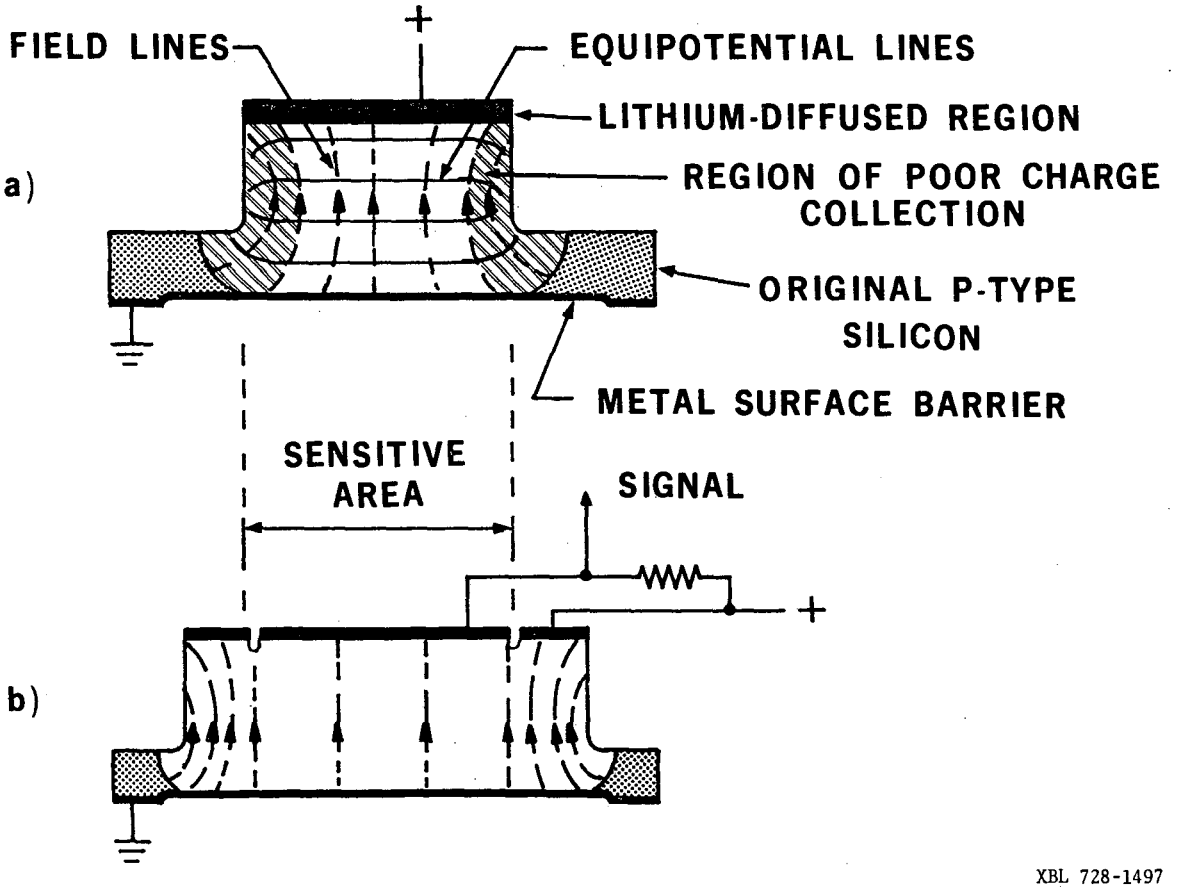
FIELD LINES
EQUIPOTENTIAL LINES
LITHIUM-DIFFUSED REGION
a)
REGION OF POOR CHARGE COLLECTION
ORIGINAL P-TYPE SILICON
METAL SURFACE BARRIER
SENSITIVE AREA
SIGNAL
b)
XBL 728-1497

Fig. 2.6

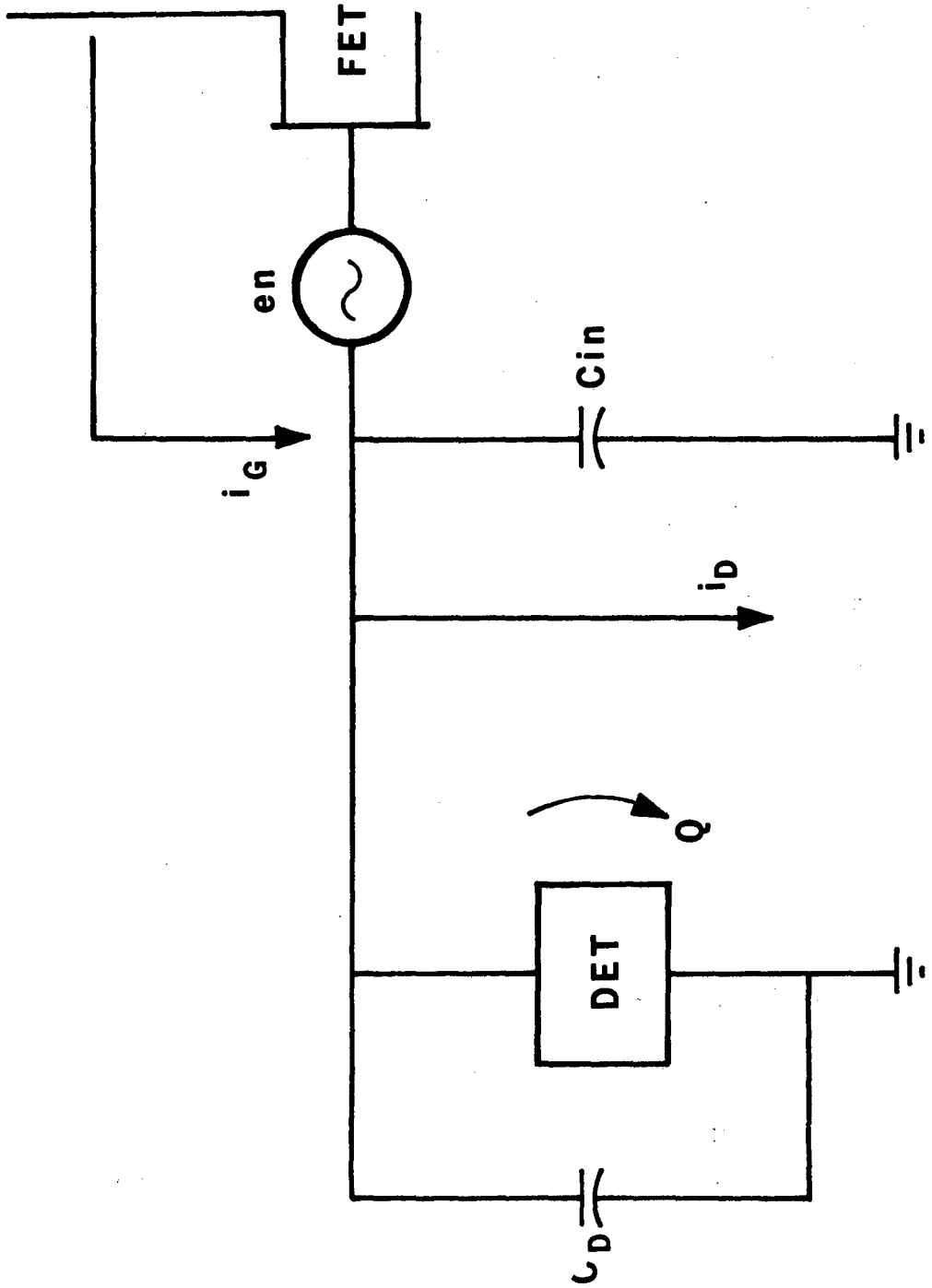

XBL 786-9325

Fig. 2.7

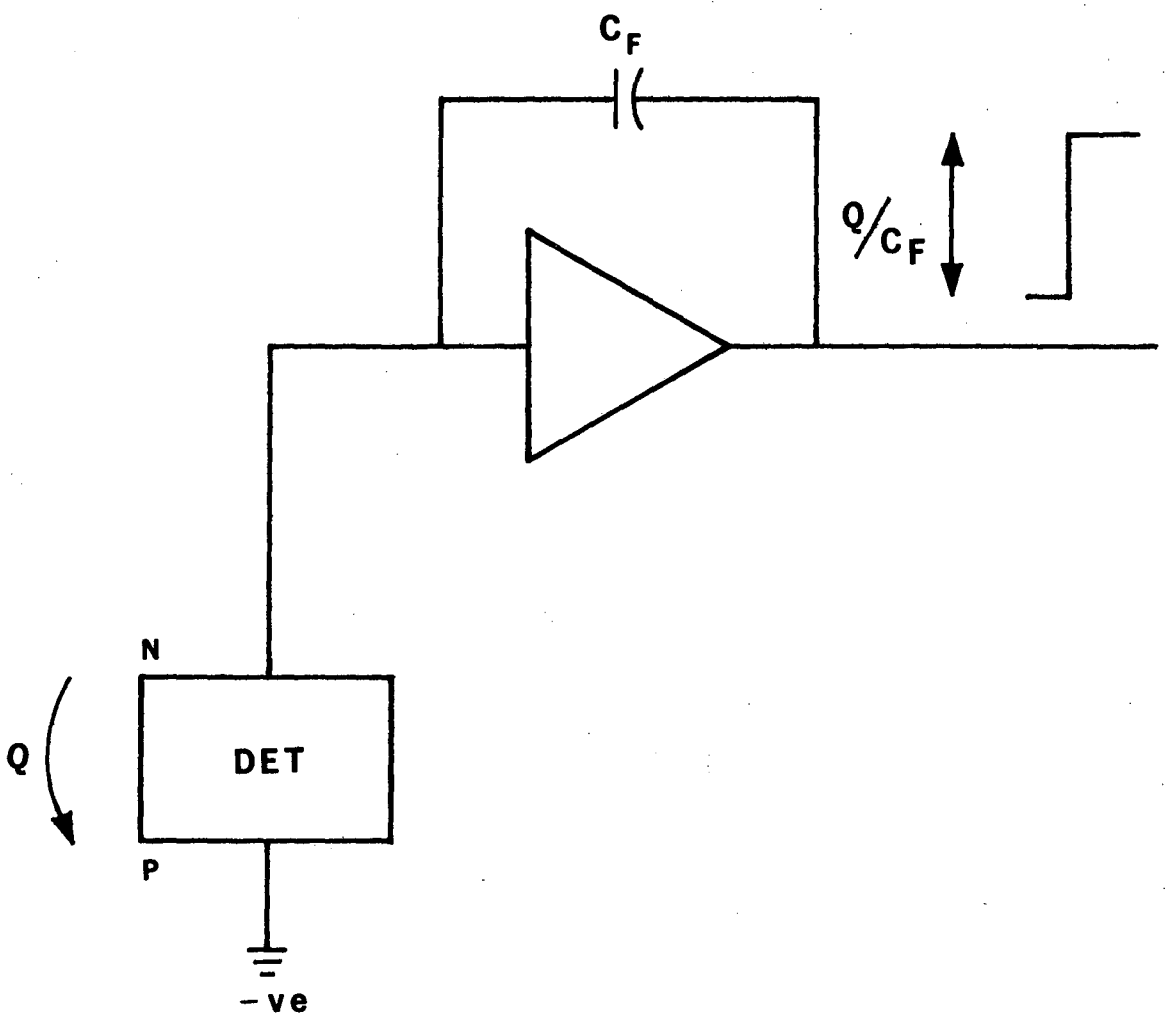

XBL 786-9327

Fig. 2.8

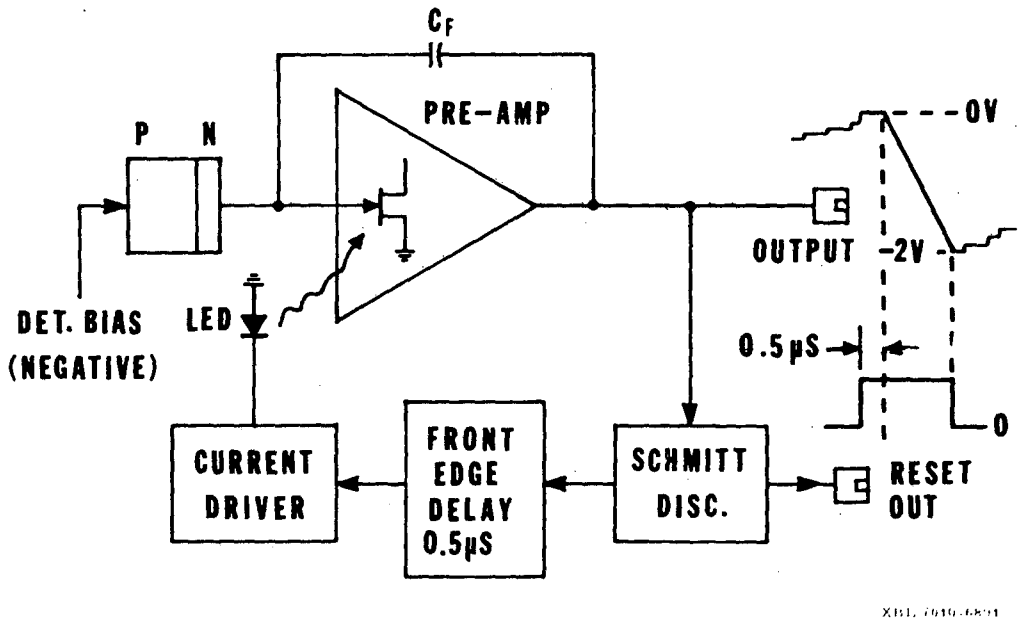
C_F
PRE-AMP
P
N
DET. BIAS
(NEGATIVE)
LED
OUTPUT
0V
-2V
0.5μS
0
CURRENT
DRIVER
FRONT
EDGE
DELAY
0.5μS
SCHMITT
DISC.
RESET
OUT

Fig. 2.9

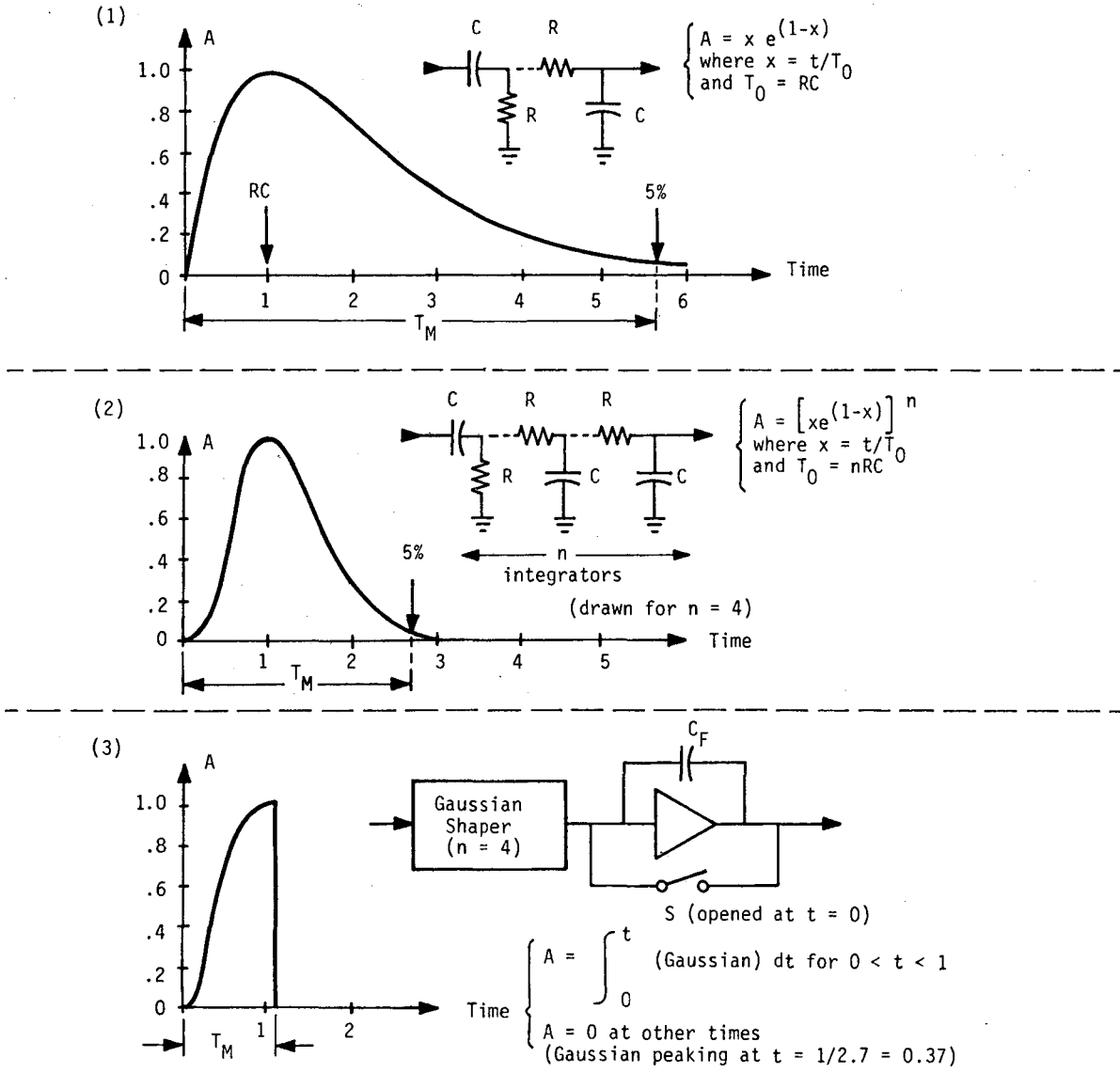

XBL 786-9336

Fig. 2.10

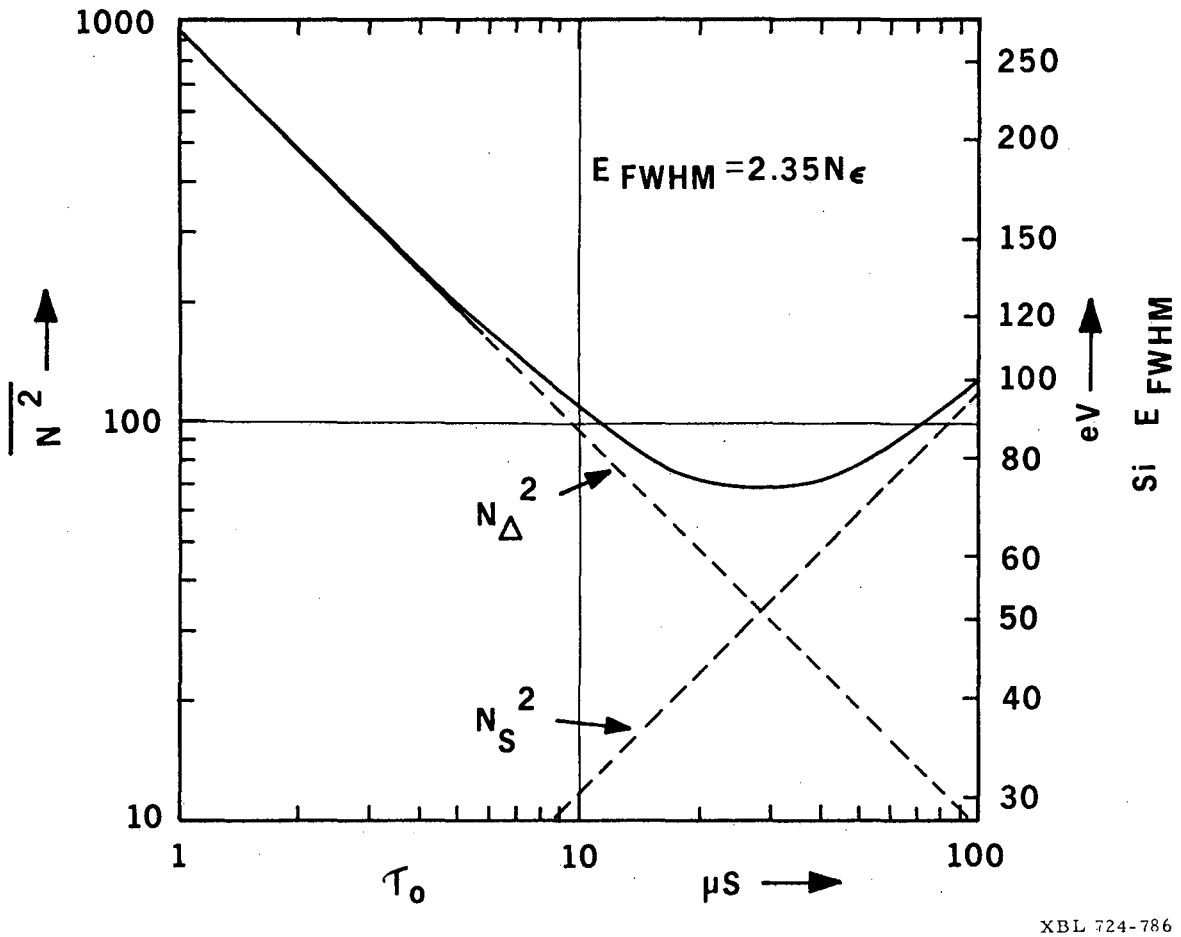
1000
100
10
1
10
100
250
200
150
120
100
80
60
50
40
30
$E_{FWHM} = 2.35N\epsilon$
N_Δ^2
N_S^2
$\overline{N^2}$
τ_0
μS
eV
Si E_{FWHM}
XBL 724-786

Fig. 2.11

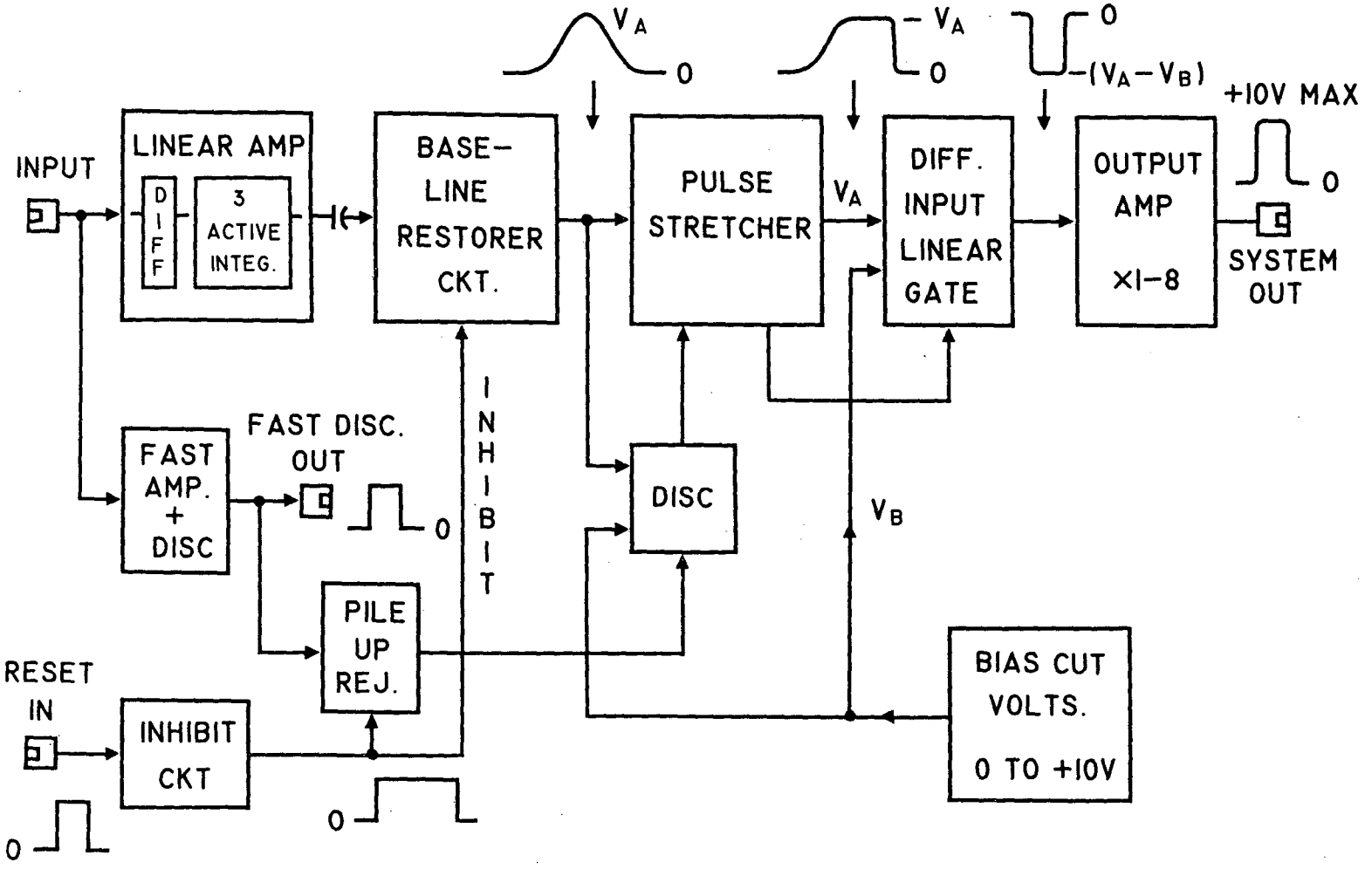

Fig. 2.12

XBL 786-9326

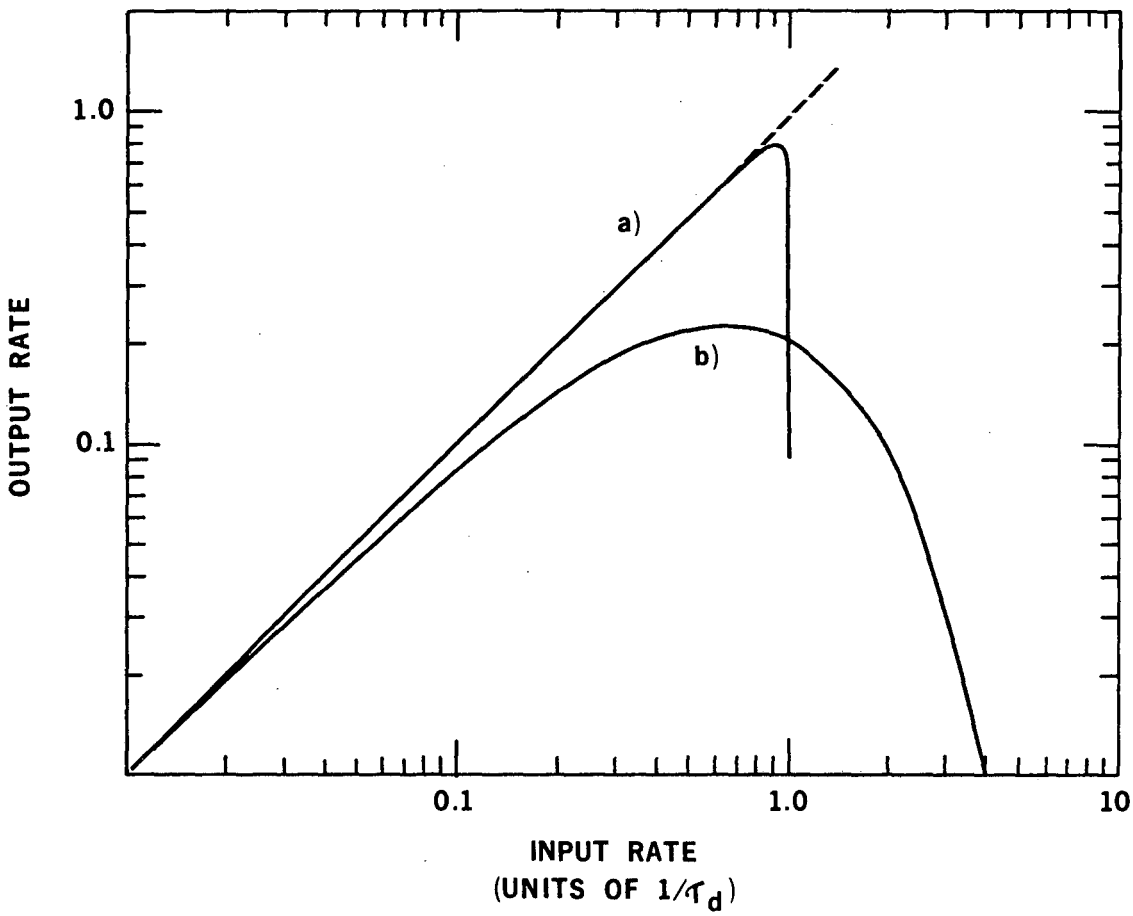

XBL 756-1685

Fig. 2.13

TECHNICAL INFORMATION DEPARTMENT
LAWRENCE BERKELEY LABORATORY
UNIVERSITY OF CALIFORNIA
BERKELEY, CALIFORNIA 94720